Progress In Electromagnetics Research, Vol. 121, 453–468, 2011

POLARIZATION CHARACTERISTICS OF A PARTIALLY COHERENT GAUSSIAN SCHELL-MODEL BEAM IN SLANT ATMOSPHERIC TURBULENCE

Y.-Q. Li, Z.-S. Wu*, and L.-G. Wang

School of Science, Xidian University, Xi'an 710071, China

Abstract—On the basis of the extended Huygens-Fresnel principle, the cross-spectral density matrix (CSDM) of partially coherent Gaussian Schell-model (GSM) beams in the slant atmospheric turbulence is derived. Given that the light emitted from a transmitter is elliptically polarized light, the degree of polarization (DoP) of the partially coherent GSM beams is represented by Stokes parameters expressed by the elements of the CSDM. The expressions of the orientation angle, polarized light intensity in the major axis are derived and the numerical results are presented. Depolarization theory is studied using a Mueller matrix and the depolarization index (DI) is obtained to describe the depolarized state of the partially coherent GSM beams propagating in the slant atmospheric turbulence. Results show that the DOP and DI of the beam tend to their initial value in the long-range propagation.

1. INTRODUCTION

Studies on light beams propagating through atmospheric turbulence are highly important for many applications such as tracking, remote sensing, and space optical communications. Aside from fully coherent Gaussian beams, the statistical properties of scalar partially coherent GSM beams propagating in atmospheric turbulence have been extensively investigated. Some scholars have recently studied partially coherent optical vortex beams propagating through atmospheric turbulence [1, 2]. Ngo and Pemha [3] investigated the propagation of a laser beam through a plane and free turbulence heated airflow. The average intensity and spread of partially coherent standard and elegant

Received 22 September 2011, Accepted 26 October 2011, Scheduled 4 November 2011

* Corresponding author: Zhen-Sen Wu (wuzhs@mail.xidian.edu.cn).

Laguerre-Gaussian beams in atmospheric turbulence were shown in [4]. The average intensity and spread of partially coherent four-petal Gaussian beams in atmospheric turbulence were also investigated [5]. Researchers from our group have studied log-amplitude variance, beam spread, wander variance, and scintillation considering the inner and outer scales of Gaussian beams propagating through slant atmospheric turbulence [6–8]. On the basis of the extended Huygens-Fresnel principle, we also studied the scattering of partially coherent GSM beams from a diffused target in the slant double-passage atmospheric turbulence [9].

A diagnosis method for articular cartilage damage using polarization-sensitive optical coherence tomography was discussed by Shyu et al. [10]. Zhu et al. [11] deal with the design, fabrication and measurement of a polarization insensitive microwave absorber based on metamaterial. The design and realization of a multi-band and polarization insensitive metamaterial absorber were presented by Huang and Chen [12]. Wolf [13, 14] proposed the unified theory of coherence and polarization, which enables the determination of changes in beam statistical properties, including spectral density, spectral coherence degree, and state of polarization (i.e., the size, shape, and orientation of the elliptically polarized light). In [15], the authors derived a generally analytical formula for the elements of the CSDM of isotropic, semi-isotropic, and anisotropic partially coherent flat-topped beams propagating in atmospheric turbulence.

Many theoretical studies on partially coherent electromagnetic beams due to using the CSDF result in simplification [16–18]. The unified theory of coherence and polarization indicates that the changes in the DoP of a light beam propagating in any linear medium are either deterministic or random. The researchers from Wolf's group [19] investigated the changes in the polarization of electromagnetic Gaussian-Schell model (EGSM) beams propagating through atmospheric turbulence. And they also studied the effects of atmospheric turbulence on the DoP of a partially coherent EGSM beam, as well as DoP behavior in the region of space where the beam and atmospheric turbulence exist simultaneously [20]. Sihvola [21] presented the depolarization factors for anisotropic metamaterials. And G. R. Lin et al. [22] observed nonlinear depolarization on randomly sub-wavelength corrugated semiconductor nano-pillar and second-order scattering induced reflection divergence. Wang and Li [23] studied the scattering from a two-dimensional (2-D) perfectly electrically conducting (PEC) cylinder partially embedded in a random dielectric rough surface interface for the case of horizontal polarization.

The depolarization of a linearly polarized laser beam was

investigated in Ref. [24] using an optical path of 4.5 km. Gil and Bernabeu [25, 26] introduced the depolarization index (DI), which features a well-defined and useful geometric meaning in the configuration space of the Mueller matrix. Two single-number metrics for the depolarization of samples were differentiated by Chipman [27]. The average DoP of the exiting light averaged over the Poincaré sphere and the DI (even though it is very often close to the average DoP) can differ by more than 0.5 for certain Mueller matrices. Zhu and Cai [28] derived analytical formula for the CSDM of a twisted electromagnetic Gaussian Schell-model (TEGSM) beam propagating through an astigmatic ABCD optical system in gain or absorbing media and studied numerically the evolution properties of the DoP of a TEGSM beam in a Gaussian cavity filled with gain media.

The aforementioned studies focused on the uses of partially coherent beams propagating in horizontal atmospheric turbulence and free space. However, the polarized light intensity and depolarized state of the beams have not been extensively studied. The present paper focuses on discussing the effects of atmospheric turbulence on the statistical polarization characteristics of partially coherent GSM beams in a slant path. We concentrate on the depolarization theory of an elliptically polarized GSM beam using a Mueller matrix and obtain the DI. It is important to study the changes in the degree of polarization of partially coherent beams propagating through atmospheric turbulence, and it has applications in free space optical communication and high power laser beam propagation in atmosphere.

2. THEORETICAL FORMULATIONS

The field propagates from the source plane $z = 0$ to the plane $z > 0$ where atmospheric turbulence exists. To describe the second-order coherence properties of the partially coherent beam, a 2×2 CSDM was introduced [20]:

$$\overleftrightarrow{W}(\vec{\rho}_1, \vec{\rho}_2; L) \equiv W_{ij}(\vec{\rho}_1, \vec{\rho}_2; L) = \left\langle E_i(\vec{\rho}_1; L) E_j^*(\vec{\rho}_2, L) \right\rangle \quad (i{=}x, y; j{=}x, y) \quad (1)$$

where $< \cdot >$ represents the ensemble average over the medium statistic, the asterisk denotes the complex conjugate, and E_i, E_j are the fields in two mutually orthogonal directions perpendicular to the propagation direction of the beam (z axis). The two mutually orthogonal transverse fields of the beam in atmospheric turbulence can be expressed using the extended Huygens-Fresnel principle:

$$E(\vec{\rho}, L) = \frac{-ik}{2\pi L} \exp(ikL) \int d\vec{r}\, E_0(\vec{r}, 0) \exp\left[\frac{ik}{2L} \left| \vec{\rho} - \vec{r} \right|^2 + \psi(\vec{r}, \vec{\rho}) \right] \quad (2)$$

where $E(\vec{\rho}, L)$ and $E_0(\vec{r}, 0)$ are the field distributions in the receiver $(\vec{\rho}, L)$ and source $(\vec{r}, 0)$ planes, respectively, and $\psi(\vec{r}, \vec{\rho})$ represents the phase perturbation determined by the properties of the medium.

Using (1) and (2), the CSDM of the partially coherent beam propagating in atmospheric turbulence is written as

$$W_{ij}(\vec{\rho}_1,\vec{\rho}_2;L)=\frac{1}{(\lambda L)^2}\iint dr_1 dr_2 W_{ij}^{(0)}(\vec{r}_1,\vec{r}_2)\left\langle \exp[\psi(\vec{r}_1,\vec{\rho}_1)+\psi^*(\vec{r}_2,\vec{\rho}_2)]\right\rangle_m \times \exp\left\{\frac{ik}{2L}\left[(\vec{\rho}_1-\vec{r}_1)^2-(\vec{\rho}_2-\vec{r}_2)^2\right]\right\} \tag{3}$$

where $k = 2\pi/\lambda$ is the optical wave number in free space, $W_{ij}^{(0)}(\vec{r}_1, \vec{r}_2)$ denotes the elements of the CSDM at source plane $z = 0$, and $\langle\rangle_m$ represents the ensemble average over the turbulence medium. In addition [29]

$$\left\langle \exp\left[\psi(\vec{r}_1,\vec{\rho}_1)+\psi^*(\vec{r}_2,\vec{\rho}_2)\right]\right\rangle_m = \exp\left[-(1/2)\,D_\psi(\vec{r}_d,\vec{\rho}_d)\right] \tag{4}$$

where $\vec{r}_d = \vec{r}_1 - \vec{r}_2$, $\vec{\rho}_d = \vec{\rho}_1 - \vec{\rho}_2$. D_ψ is the phase structure function, which is written as [30]

$$D_\psi = 2.92k^2 L\int_0^1 dt C_n^2(tL)\left|\vec{r}_d t+(1-t)\vec{\rho}_d\right|^{5/3} \cong 2\left[\left(r_d^2+\vec{r}_d\cdot\vec{\rho}_d+\rho_d^2\right)/\rho_T^2\right] \tag{5}$$

where $\rho_T = [1.46k^2 L\int_0^1 C_n^2(\xi L)(1-\xi)^{5/3}d\xi]^{-3/5}$ is the coherence length of a spherical wave propagating in the slant atmospheric turbulence and $C_n^2(\xi L)$ is the refractive index structure constant of the atmosphere obtained by the International Telecommunication Union [31].

Using (4) and (5), let $\vec{\rho}_1 = \vec{\rho}_2 = \vec{\rho}$, we obtain

$$\left\langle \exp\left[\psi\left(\vec{r}_1,\vec{\rho}\right)+\psi^*\left(\vec{r}_2,\vec{\rho}\right)\right]\right\rangle_m \cong \exp\left[-r_d^2/\rho_T^2\right] \tag{6}$$

For the GSM beams, the CSDM in source plane $z = 0$ has the elements [32]

$$W_{ij}^{(0)}(\vec{r}_1,\vec{r}_2)=A_i A_j B_{ij}\exp\left[-\left(\frac{r_1^2}{4\sigma_i^2}+\frac{r_2^2}{4\sigma_j^2}\right)\right]\exp\left[-\frac{(\vec{r}_2-\vec{r}_1)^2}{2\delta_{ij}}\right] \tag{7}$$

where A_i, A_j, B_{ij} are the coefficients and σ_i^2, σ_j^2 are the waist sizes of an elliptical Gaussian beam in the x and y directions, respectively. δ_{ij} is the coherence length of the source at plane $z = 0$. Parameters A_i, B_{ij}, σ_i, δ_{ij} are independent of position and satisfy the following expressions [32]:

$$B_{ij} = 1 \;\; (i = j), \;\; |B_{ij}| \le 1 \;\; (i \ne j), \;\; B_{ij} = B_{ji}^*, \;\; \text{and} \;\; \delta_{ij} = \delta_{ji} \tag{8}$$

where $B_{xy} = B_{yx}^* = a\exp(i\phi)$, a is the amplitude, and ϕ is the phase delay of the electric vector in the y direction relative to the x direction.

$$W_{ij}(\vec{\rho},\vec{\rho};L) = \frac{A_iA_jB_{ij}}{(\lambda L)^2}\iint d\vec{r}_1 d\vec{r}_2 \exp\left[-\left(\frac{r_1^2}{4\sigma_i^2}+\frac{r_2^2}{4\sigma_j^2}\right)\right]\exp\left[-\frac{(\vec{r}_2-\vec{r}_1)^2}{2\delta_{ij}}\right] \times \left\langle \exp\left[\psi\left(\vec{r}_1,\vec{\rho}\right)+\psi^*\left(\vec{r}_2,\vec{\rho}\right)\right]\right\rangle_m \exp\left\{\frac{ik}{2L}\left[\left(\vec{\rho}-\vec{r}_1\right)^2-\left(\vec{\rho}-\vec{r}_2\right)^2\right]\right\} \quad (9)$$

In the conversion of coordinate $\vec{r}_c = (\vec{r}_1+\vec{r}_2)/2$, we obtain

$$W_{ij}(\vec{\rho},\vec{\rho};L) = \frac{A_iA_jB_{ij}}{(\lambda L)^2}\iint d\vec{r}_d d\vec{r}_c \exp\left[-\frac{1}{4\sigma_i^2}\left(r_c^2+\vec{r}_d\cdot\vec{r}_c+\frac{1}{4}r_d^2\right) -\frac{1}{4\sigma_j^2}\left(r_c^2-\vec{r}_d\cdot\vec{r}_c+\frac{1}{4}r_d^2\right)\right]\times\exp\left[-\frac{r_d^2}{2\delta_{ij}}\right] \exp\left[-r_d^2/\rho_T^2\right]\exp\left[\frac{ik}{L}\left(-\vec{\rho}_d\cdot\vec{r}_d+\vec{r}_d\cdot\vec{r}_c\right)\right] \quad (10)$$

By integration, (10) is obtained as follows:

$$W_{ij}(\vec{\rho},\vec{\rho};L) = \frac{A_iA_jB_{ij}}{(\lambda L)^2}\cdot\frac{\pi}{\sqrt{\alpha_{ij}\chi_{ij}}}\exp\left[-\frac{\rho^2}{\Delta_{ij}^2}\right] \quad (11)$$

where

$$\alpha_{ij} = \frac{1}{16\sigma_i^2}+\frac{1}{16\sigma_j^2}+\frac{1}{2\delta_{ij}}+\frac{1}{\rho_T^2},$$
$$\chi_{ij} = \left(\frac{1}{4\sigma_i^2}+\frac{1}{4\sigma_j^2}-\frac{\beta_{ij}^2}{\alpha_{ij}}+\frac{k^2}{4\alpha_{ij}L^2}\right)+i\frac{\beta_{ij}k}{\alpha_{ij}L} \quad (12)$$
$$\beta_{ij} = \frac{1}{8}\left(\frac{1}{\sigma_i^2}-\frac{1}{\sigma_j^2}\right),\ \Delta_{ij} = \frac{2}{k}\sqrt{\left(L^2-\frac{k^2}{4\alpha_{ij}\chi_{ij}}+\frac{L^2}{\alpha_{ij}\chi_{ij}}\right)-i\frac{kL}{\alpha_{ij}\chi_{ij}}}$$

The polarization matrix of the partially coherent GSM beams in the slant atmospheric turbulence is represented in the form

$$W = \begin{pmatrix} W_{xx}W_{xy} \\ W_{yx}W_{yy} \end{pmatrix} \quad (13)$$

where the elements W_{xx}, W_{yy}, W_{xy}, W_{yx} in matrix W are given by (11). For an elliptically polarized beam, the two diagonal elements W_{xx}, W_{yy} are real quantities. The two off-diagonal elements W_{xy}, W_{yx} are complex quantities, which are conjugated with each other. If W_{xy}, W_{yx} are real quantities (i.e., $W_{xy} = W_{yx}$), the beams become linearly polarized light.

2.1. Degree of Polarization

The Stokes parameters, which include DoP information, can be expressed in terms of the elements of the CSDM using the following formulas [32]:

$$\begin{aligned} s_0'&=W_{xx}(\vec{\rho},\vec{\rho},L)+W_{yy}(\vec{\rho},\vec{\rho},L),\ s_1'=W_{xx}(\vec{\rho},\vec{\rho},L)-W_{yy}(\vec{\rho},\vec{\rho},L)\\ s_2'&=W_{xy}(\vec{\rho},\vec{\rho},L)+W_{yx}(\vec{\rho},\vec{\rho},L),\ s_3'=i\left[W_{yx}(\vec{\rho},\vec{\rho},L)-W_{xy}(\vec{\rho},\vec{\rho},L)\right] \end{aligned} \tag{14}$$

Using (7) and (14), the Stokes parameters and DoP in source plane $z = 0$ can be expressed as

$$\begin{aligned} s_0 &= A_x^2 \exp\left(-\frac{\rho^2}{2\sigma_x^2}\right) + A_y^2 \exp\left(-\frac{\rho^2}{2\sigma_y^2}\right)\\ s_1 &= A_x^2 \exp\left(-\frac{\rho^2}{2\sigma_x^2}\right) - A_y^2 \exp\left(-\frac{\rho^2}{2\sigma_y^2}\right)\\ s_2 &= 2A_xA_y \cdot \mathrm{Re}\left[B_{xy}\right] \exp\left[-\frac{\rho^2}{4}\left(\frac{1}{\sigma_x^2}+\frac{1}{\sigma_y^2}\right)\right]\\ s_3 &= 2A_xA_y \cdot \mathrm{Im}\left[B_{xy}\right] \exp\left[-\frac{\rho^2}{4}\left(\frac{1}{\sigma_x^2}+\frac{1}{\sigma_y^2}\right)\right] \end{aligned} \tag{15}$$

$$P_0(\vec{\rho},L) = \sqrt{s_1^2+s_2^2+s_3^2}/s_0 \tag{16}$$

Using (11) and (14), the Stokes parameters and DoP in the plane $z > 0$ are given by

$$\begin{aligned} s_0' &= \frac{A_x^2}{\sqrt{\alpha_{xx}\chi_{xx}}} \exp\left(-\frac{\rho^2}{\Delta_{yy}^2}\right) + \frac{A_y^2}{\sqrt{\alpha_{yy}\chi_{yy}}} \exp\left(-\frac{\rho^2}{\Delta_{yy}^2}\right)\\ s_1' &= \frac{A_x^2}{\sqrt{\alpha_{xx}\chi_{xx}}} \exp\left(-\frac{\rho^2}{\Delta_{xx}^2}\right) - \frac{A_y^2}{\sqrt{\alpha_{yy}\chi_{yy}}} \exp\left(-\frac{\rho^2}{\Delta_{yy}^2}\right)\\ s_2' &= \frac{A_xA_yB_{xy}}{\sqrt{\alpha_{xy}\chi_{xy}}} \exp\left(-\frac{\rho^2}{\Delta_{xy}^2}\right) + \frac{A_xA_yB_{yx}}{\sqrt{\alpha_{yx}\chi_{yx}}} \exp\left(-\frac{\rho^2}{\Delta_{yx}^2}\right)\\ s_3' &= i\left[\frac{A_xA_yB_{yx}}{\sqrt{\alpha_{yx}\chi_{yx}}} \exp\left(-\frac{\rho^2}{\Delta_{yx}^2}\right) - \frac{A_xA_yB_{xy}}{\sqrt{\alpha_{xy}\chi_{xy}}} \exp\left(-\frac{\rho^2}{\Delta_{xy}^2}\right)\right] \end{aligned} \tag{17}$$

$$P(\vec{\rho},L) = \sqrt{s'^2_1+s'^2_2+s'^2_3}/s_0' \tag{18}$$

In this paper, the following parameters are used: $B_{xy} = 0.5\exp(i\pi/3)$, $\delta_{xy} = \delta_{yx} = 4\,\mathrm{mm}$, and $\delta_{xx} = 1\,\mathrm{mm}$, $\delta_{yy} = 2\,\mathrm{mm}$. Source polarized light intensity ratio $I_x/I_y = A_x^2/A_y^2$. The influence of spot

sizes, wavelengths, and propagation heights on the DoP is depicted in Figures 1–4.

Figure 1 shows that when $L > 100$ m, with increasing propagation distance, the variation trends of the DoP of the beams with $I_x/I_y \leq 1$ differ from that of the DoP of the beams with $I_x/I_y > 1$. For $I_x/I_y > 1$, the greater the ratio, the larger the DoP is, but for $I_x/I_y < 1$, the greater the ratio, the smaller the DoP is. The variation trends in Figure 1 are similar particularly to Figure 6 in [20] for $I_x/I_y < 1$. The variation trends of the DoP of the beams with $I_x/I_y = 1$ (circularly polarized light) and $I_x/I_y < 1$ are also similar, and the variation in the DoP is clearly observable at a moderate turbulence level, in which phase perturbation is dominant. In short-range propagation, the strength of turbulence is negligible. Hence, the DoPs of the beams with source polarized light intensity ratios of 4 and 1/4 or 8 and 1/8 are almost identical at 200 m (at a weak turbulence level). The results differ considerably in the range 200 m–10 km (at a moderate turbulence level).

Figure 2 shows that at a certain distance (about at 10–30 km), the DoP reaches its maximum value. The DoP of the beams with $I_x/I_y = 1/2$ is greater than that of the beams with $I_x/I_y = 2$. At $I_x/I_y > 1$, a greater ratio indicates a larger DoP. When the propagation distance is greater than 10 km, a larger the spot size yields a greater DoP. In the range 100–500 m (at a weak turbulence level), the influence of spot size on the DoP is minimal. If the spot size is smaller than or equal to 1 cm, the variation in the DoP of the beams is imperceptible when the propagation distance is greater than 2 km. However, the variation in the DoP visibly changes when the spot size is greater than 1 cm.

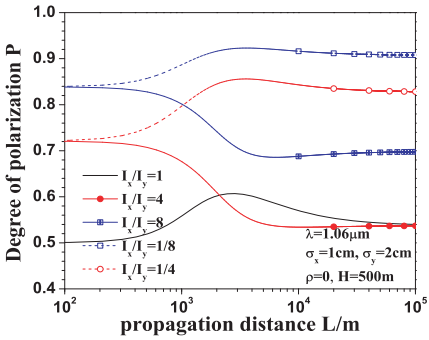

Figure 1. DoP versus propagation distance L for different source polarized light intensity ratios.

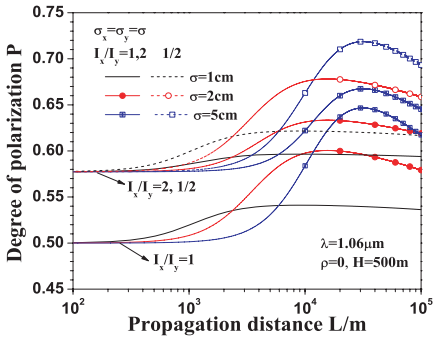

Figure 2. DoP versus propagation distance L for different spot sizes.

Figure 3 shows that the variations in the DoP are clearly observable at a moderate turbulence level (in the range 1–10 km) because phase perturbation is dominant. A larger wavelength indicates a greater DoP, and the influence of wavelength on the DoP is large. Figure 3(a) illustrates that at a 3.5 km distance, the DoP of the beams with $I_x/I_y = 1$ (circularly polarized light) reaches its maximum. In Figure 3(b), the variation trend of the DoP of beams with $I_x/I_y = 2$ differs from that of the DoP of beams with $I_x/I_y = 1/2$. Moreover, the variation in the beams with $I_x/I_y = 1/2$ is almost monotonic.

As shown in Figure 4, the shapes of light spots and source polarized light intensity ratios influence the variation trends of the

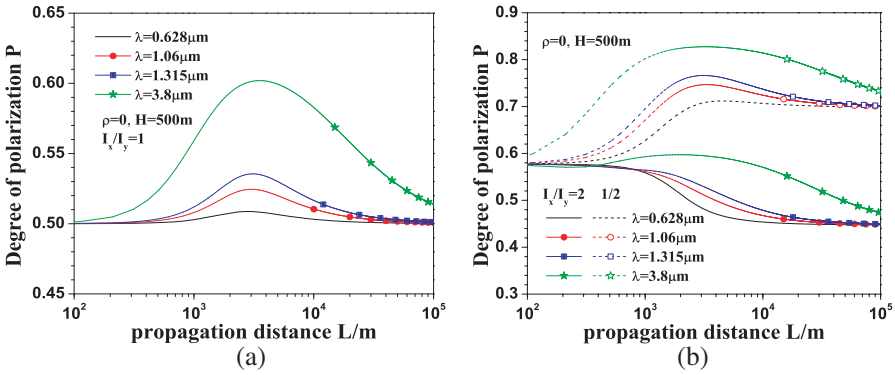

Figure 3. DoP versus propagation distance L for different wavelengths. (a) $\sigma_x = \sigma_y = 2\,\text{cm}$, (b) $\sigma_x = 1\,\text{cm}$, $\sigma_y = 2\,\text{cm}$.

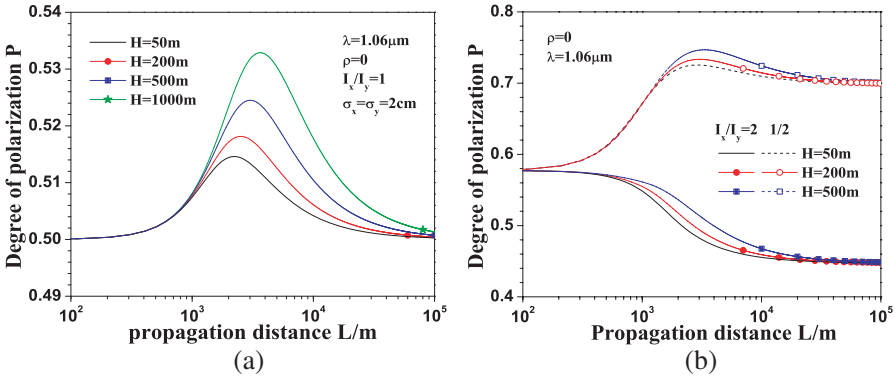

Figure 4. DoP versus propagation distance L for different receiving heights. (a) $\sigma_x = \sigma_y = 2\,\text{cm}$, (b) $\sigma_x = 1\,\text{cm}$, $\sigma_y = 2\,\text{cm}$.

DoP with increasing propagation distance. Figure 4(a) shows that with $\sigma_x = \sigma_y = 2\,\text{cm}$ (the shape of the light spot is circular) and at a 3.5 km distance, the DoP reaches its maximum, similar to that observed in Figure 3(a). In sufficiently short- and long-range propagation, the strength of the turbulence is negligible and overcomes the change in polarization caused by phase perturbation. Hence, the DoP value is small. Figure 4(b) illustrates that with $\sigma_x = 1\,\text{cm}$, $\sigma_y = 2\,\text{cm}$ (the shape of the light spot is elliptical), the DoP differs from that in Figure 4(a). The variation trend of the DoP of the beams with $I_x/I_y = 2$ differs from that of the DoP of the beams with $I_x/I_y = 1/2$. The variation of the beams with $I_x/I_y = 1/2$ is also monotonic. Figure 4 shows the smaller the receiving height, the larger the DoP is.

2.2. Orientation Angle

Orientation angle θ_0 is the smallest angle that the major axis of the polarization ellipse creates with the x direction. Therefore, the x and y coordinate system is rotated counterclockwise with respect to the positive z direction, and is presented using the following formula [15]:

$$\theta_0\left(\vec{\rho}, L\right) = \frac{1}{2}\arctan\left(\frac{2\text{Re}\left[W_{xy}\left(\vec{\rho}, L\right)\right]}{W_{xx}\left(\vec{\rho}, L\right) - W_{yy}\left(\vec{\rho}, L\right)}\right) \tag{19}$$

Substituting (11) into (19) yields

$$\theta_0\left(\vec{\rho}, L\right) = \frac{1}{2}\arctan\left\{\frac{2\text{Re}\left[\frac{A_x A_y B_{xy}}{\sqrt{\alpha_{xy}\chi_{xy}}}\exp\left(-\frac{\rho^2}{\Delta_{xy}^2}\right)\right]}{\frac{A_x^2}{\sqrt{\alpha_{xx}\chi_{xx}}}\exp\left(-\frac{\rho^2}{\Delta_{xx}^2}\right) - \frac{A_y^2}{\sqrt{\alpha_{yy}\chi_{yy}}}\exp\left(-\frac{\rho^2}{\Delta_{yy}^2}\right)}\right\} \tag{20}$$

When the spot is elliptical, the value of orientation angle does not equal zero, this value is zero at a weak turbulence level (in the range 100 m–1 km) when the spot is circular (Figure 5). The orientation angle visibly changes at a moderate turbulence level (in the range 1–10 km), in which the orientation angle reaches its maximum. The orientation angle with $\rho > 0$ (considering beam expansion) is smaller than that with $\rho = 0$. The variation in orientation angle of the beams with $\rho > 0$ is more rapid than that of the beams with $\rho = 0$ at a moderate turbulence level. This variation speed is due to the influence of beam expansion on the orientation angle. When the propagation distance is greater than 15 km, the influence of transverse distance ρ on the polarized orientation angle is minimal, and the orientation angle no longer varies with increasing propagation distance.

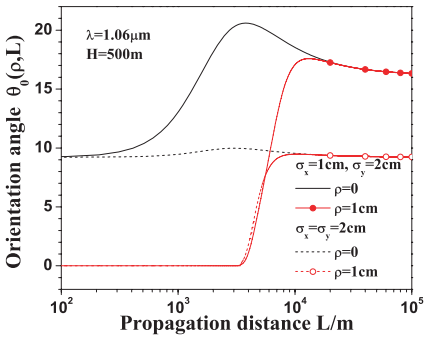

Figure 5. Orientation angle versus propagation distance L for different spot sizes and transverse distances ($A_x = 2$, $A_y = 1$).

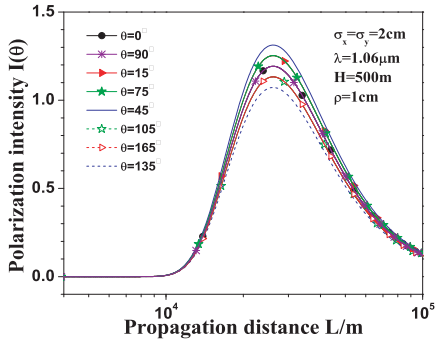

Figure 6. Polarized intensity versus propagation distance L for different orientation angles ($A_x = 2$, $A_y = 1$).

2.3. Polarized Light Intensity in the Major Axis Direction

The orientation angle is the separation angle between the x axis and major axis of the polarization ellipse, the electrical field in the major axis direction is written as

$$E(\theta) = E_x \cos\theta + E_y \sin\theta \tag{21}$$

Thus, the polarized light intensity in the major axis direction is obtained:

$$\begin{aligned} I(\theta) &= \langle E(\theta)E^*(\theta)\rangle = \left\langle (E_x\cos\theta + E_y\sin\theta)\cdot\left(E_x^*\cos\theta + E_y^*\sin\theta\right)\right\rangle \\ &= \frac{\pi}{(\lambda L)^2}\left\{\frac{A_x^2}{\sqrt{\alpha_{xx}\chi_{xx}}}\exp\left(-\frac{\rho^2}{\Delta_{xx}^2}\right) + \frac{A_y^2}{\sqrt{\alpha_{yy}\chi_{yy}}}\exp\left(-\frac{\rho^2}{\Delta_{yy}^2}\right)\right. \\ &\quad \left. +2\sin\theta\cos\theta\mathrm{Re}\left[\frac{A_xA_yB_{xy}}{\sqrt{\alpha_{xy}\chi_{xy}}}\exp\left(-\frac{\rho^2}{\Delta_{xy}^2}\right)\right]\right\} \end{aligned} \tag{22}$$

where Re represents the real part derivation.

Figure 6 shows that in the range 10–100 km, the variation in polarized intensity is clearly observable and at a 26.5 km distance, polarized intensity reaches its maximum value. When the polarized orientation angles are 0° and 90°, 15° and 75°, 105° and 165°, respectively, the values of polarized intensity are identical. The intensity with a 45° orientation angle is greater than that with 135° one. The polarized intensities of two symmetrical orientation angles at 45° or 135° (15° and 75°, or 105° and 165°) are identical. The polarized

intensity of two symmetrical orientation angles at 45° (in the range 0°–90°) is greater than that of the two symmetrical orientation angles at 135° (90°–180°).

3. DEPOLARIZATION THEORY

3.1. Mueller Matrices

Assuming that an incident light interacts linearly with atmospheric turbulence, the polarization-transformation properties of the incident light are described by a Mueller matrix $\overleftrightarrow{M}$ that is associated with incident Stokes vector $\overleftrightarrow{S}_{\text{incident}}$ and exiting Stokes vector $\overleftrightarrow{S}_{\text{Exiting}}$ by [27]

$$\overleftrightarrow{S}_{\text{Exiting}} = \overleftrightarrow{M} \cdot \overleftrightarrow{S}_{\text{incident}} = \begin{bmatrix} M_{00} & M_{01} & M_{02} & M_{03} \\ M_{10} & M_{11} & M_{12} & M_{13} \\ M_{20} & M_{21} & M_{22} & M_{23} \\ M_{30} & M_{31} & M_{32} & M_{33} \end{bmatrix} \cdot \begin{bmatrix} S_0 \\ S_1 \\ S_2 \\ S_3 \end{bmatrix} = \begin{bmatrix} S'_0 \\ S'_1 \\ S'_2 \\ S'_3 \end{bmatrix} \quad (23)$$

The Mueller matrix contains 16 degrees of freedom (DOFs), in which seven DOFs are nondepolarization factors caused by diattenuation, retardance, and polarization-independent loss such as absorption. The other nine DOFs are depolarization factors that describe how different states of polarization are depolarized.

In atmospheric turbulence, depolarization occurs when the DoP of the exiting beam is less than that of the incident beam. The reduction in the DoP (depolarization phenomenon) assumes the entire range from 0% (no depolarization) to 100% (complete depolarization).

Using (14), (15), and (23), we represent the Mueller matrix of the ellipse polarization in slant atmospheric turbulence as

$$\overleftrightarrow{M} = \begin{bmatrix} 1 & a & 0 & 0 \\ b & c & 0 & 0 \\ 0 & 0 & d & e \\ 0 & 0 & f & g \end{bmatrix} \quad (24)$$

Let $\rho = 0$. The elements of the Mueller matrix are calculated as

$$\begin{aligned} a &= c = \frac{1}{2}\left(\frac{1}{\sqrt{\alpha_{xx}\chi_{xx}}} - \frac{1}{\sqrt{\alpha_{yy}\chi_{yy}}}\right) \quad b = \frac{1}{2}\left(\frac{1}{\sqrt{\alpha_{xx}\chi_{xx}}} + \frac{1}{\sqrt{\alpha_{yy}\chi_{yy}}}\right) \\ d &= g = \frac{1}{2}\left(\frac{1}{\sqrt{\alpha_{xy}\chi_{xy}}} + \frac{1}{\sqrt{\alpha_{yx}\chi_{yx}}}\right) \quad e = -f = \frac{i}{2}\left(\frac{1}{\sqrt{\alpha_{xy}\chi_{xy}}} - \frac{1}{\sqrt{\alpha_{yx}\chi_{yx}}}\right) \end{aligned} \quad (25)$$

Equation (25) shows that the Mueller matrix is associated with incident wavelength, spot size, coherence length, and propagation height. Thus, the depolarized state varies with incident-polarized states.

3.2. Depolarization Index

The DI as a single number metric for characterizing the depolarization of a Muller matrix was proposed in [26]. It is defined as

$$\mathrm{DI}\left[\overleftrightarrow{M}\right] = \frac{\left(\sum_{i,j=0}^{3} M_{i,j}^2 - M_{00}^2\right)^{1/2}}{\sqrt{3}M_{00}} \tag{26}$$

DI = 1 corresponds to non-depolarizing Mueller matrices and DI = 0 corresponds to an ideal depolarizer. The numerator represents the Euclidean distance from the ideal depolarizer to the non-depolarizing Mueller matrix. The denominator represents the radius of the hyperspherical surface of non-depolarizing Mueller matrices for M_{00}.

Using (24) and (26), the DI is obtained as follows:

$$\mathrm{DI}\left[\overleftrightarrow{M}\right] = \frac{\left(2a^2 + b^2 + 2d^2 + 2e^2\right)^{1/2}}{\sqrt{3}M_{00}} \tag{27}$$

When a DI is greater than one or less than zero, a nonphysical Mueller matrix is represented. In practice, nonphysical Mueller matrices are occasionally elicited by measurement error, calibration error, and noise.

Figure 7(a) shows that the higher the receiving height, the larger the DI is. The peak value of the DI corresponds to a greater slant propagation distance when the receiving heights are large. As shown in Figure 7(b), the greater the spot size, the larger the DI

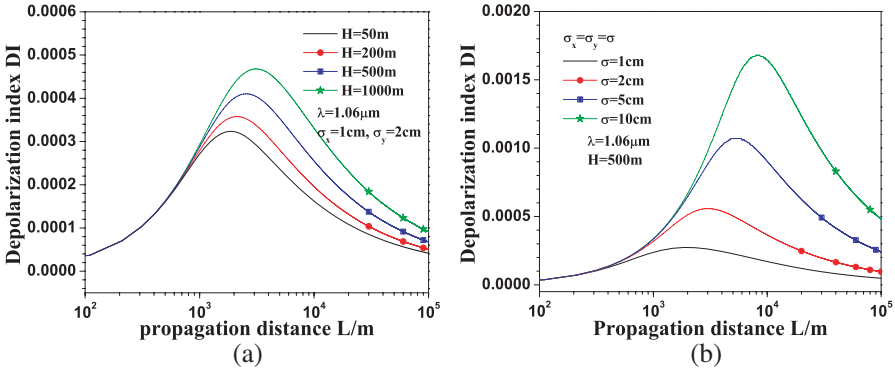

Figure 7. DI versus propagation distance L for different (a) receiving heights and (b) spot sizes.

is, and the maximum DI visibly increases. The propagation distance corresponding to the peak value of the DI shifts to a larger value as spot sizes increase. As seen in Figures 7(a) and 7(b), the influence of spot size on the DI is greater than that of the receiving height. The variation in the DI is clearly observable at a moderate turbulence level (1–10 km), in which phase perturbation is dominant. In sufficiently short-and long-range propagation, the strength of turbulence is negligible and overcomes the change in the DI caused by phase perturbation. Thus, the value of DI approaches zero; i.e., no depolarization phenomenon is generated at weak and strong turbulence levels.

4. CONCLUSION

In this study, the CSDM of partially coherent GSM beams in slant atmospheric turbulence is derived. The DoP, orientation angle, and polarized light intensity in the major axis are also derived. In addition, DI is obtained to describe the depolarized state of partially coherent GSM beams. Phase fluctuation is considered and the DoP, orientation angle, and polarized light intensity exhibit a rapid variation trend at a moderate turbulence level because of dominant phase perturbation. The conclusions are summarized as follows:

(1) The source polarized light intensity ratio, which can be both greater and less than one, influences the variation trend of the DoP as a function of propagation distance. (2) The shapes of light spot can influence the variation trend of the DoP as a function of propagation distance; the smaller the receiving height, the larger the DoP is. (3) In the range 1–10 km (at a moderate turbulence level), the variations in the DoP, orientation angle, polarized light intensity, and DI are clearly observable. (4) At a certain distance, the DI reaches its maximum value. The larger the receiving height and spot size, the greater the DI is. At 100 m–1 km and at greater than 100 km, the DI equals zero and generates no depolarization. (5) The wavelength, receiving height and light spot size can influent the values of the DoP, orientation angle, polarized light intensity, and DI.

ACKNOWLEDGMENT

This paper is supported by Fundamental Research Funds for the Central Universities and National Natural Science Foundation of China (Grant No 61172031).

REFERENCES

1. Zhang, Y. X., M. X. Tang, and C. K. Tao, "Partially coherent vortex beams propagation in a turbulent atmosphere," *Chin. Opt. Lett.*, Vol. 3, 559–561, 2005.
2. Li, J. H., H. R. Zhang, and B. D. Lu, "Partially coherent vortex beams propagating through atmospheric turbulence and coherence vortex evolution," *Optics & Laser Technology*, Vol. 42, 428–433, 2010.
3. Ngo Nyobe, E. and E. Pemha, "Propagation of a laser beam through a plane and free turbulent heated air flow: Determination of the stochastic characteristics of the laser beam random direction and some experimental results," *Progress In Electromagnetics Research*, Vol. 53, 31–53, 2005.
4. Wang, F., Y. Cai, H. T. Eyyuboglu, and Y. K. Baykal, "Average intensity and spreading of partially coherent standard and elegant Laguerre-Gaussian beams in turbulent atmosphere," *Progress In Electromagnetics Research*, Vol. 103, 33–56, 2010.
5. Li, J., Y. Chen, S. Xu, Y. Wang, M. Zhou, Q. Zhao, Y. Xin, and F. Chen, "Average intensity and spreading of partially coherent four-petal Gaussian beams in turbulent atmosphere," *Progress In Electromagnetics B*, Vol. 24, 241–261, 2010.
6. Wei, H. Y. and Z. S. Wu, "Study on the effect of laser beam propagation on the slant path through atmospheric turbulence," *Joural of Electromagnetic Waves and Applications*, Vol. 22, Nos. 5–6, 787–802, 2008.
7. Wei, H.-Y., Z.-S. Wu, and Q. Ma, "Log-amplitude variance of laser beam propagation the slant path through turbulent atmosphere," *Progress In Elenctromagnetics Research*, Vol. 108, 277–291, 2010.
8. Wu, Z.-S., H.-Y. Wei, R.-K. Yang, and L.-X. Guo, "Study on scintillation considering inner- and outer-scales for laser beam propagation on the slant path through the atmospheric turbulence," *Progress In Electromagnetics Research*, Vol. 80, 277–293, 2008.
9. Wu, Z.-S. and Y.-Q. Li, "Scattering of a partially coherent Gaussian-Schell beam from a diffuse target in slant atmospheric turbulence," *J. Opt. Soc. Am. A*, Vol. 25, 2011.
10. Shyu, J.-J., C.-H. Chan, M.-W. Hsiung, P.-N. Yang, H.-W. Chen, and W.-C. Kuo, "Diagnosis of articular cartilage damage by polarization sensitive optical coherence tomography and the extracted optical properties," *Progress In Electromagnetics Research,* Vol. 91, 365–376, 2009.

11. Zhu, B., Z. Wang, C. Huang, Y. Feng, J. Zhao, and T. Jing, "Polarization insensitive metamaterial absorber with wide incident angle," *Progress In Electromagnetics Research*, Vol. 101, 231–239, 2010.
12. Huang, L. and H. Chen, "Multi-band and polarization insensitive metamaterial absorber," *Progress In Electromagnetics Research*, Vol. 113, 103–110, 2011.
13. Korotkova, O. and E. Wolf, "Changes in the state of polarization of a random electromagnetic beam on propagation," *J. Opt. Commun.*, Vol. 246, 35–43, 2005.
14. Wolf, E., "Unified theory of coherence and polarization of random electromagnetic beams," *J. Phys. Lett.*, Vol. A312, 263–267, 2003.
15. Ghafary, B. and M. Alavinejad, "Changes in the state of polarization of partially coherent flat-topped beam in turbulent atmosphere for different source conditions," *J. Appl. Phys. B*, Vol. 102, 945–952, 2011.
16. Gori, F., M. Santarsiero, S. Vicalvi, R. Borghi, and G. Guattari, "Beam coherence polarization matrix," *Pure Appl. Opt.*, Vol. 7, 941–951, 1998.
17. Gori, F., M. Santarsiero, G. Piquero, A. Mondello, and R. Simon, "Partially polarized Gaussian Schell-model beams," *J. Opt. A: Pure Appl. Opt.*, Vol. 3, 1–9, 2001.
18. Cai, Y., D. Ge, and Q. Lin, "Fractional fourier transform for partially coherent and partially polarized Gaussian Schell-model beams," *J. Opt. A: Pure Appl. Opt.*, Vol. 5, 453–459, 2003.
19. Korotkova, O., M. Salem, and E. Wolf, "The far zone behavior of the degree of polarization of electromagnetic beams propagating through atmospheric turbulence," *J. Opt. Commun.*, Vol. 233, 225–230, 2004.
20. Salem, M., O. Korotkova, A. Dogariu, and E. Wolf, "Polarization changes in partially coherent electromagnetic beams propagating through turbulence atmosphere," *Waves in Random Media*, Vol. 14, 513–523, 2004.
21. Sihvola, A., "Metamaterials and depolarization factors," *Progress In Electromagnetics Research*, Vol. 51, 65–82, 2005.
22. Lin, G.-R., F.-S. Meng, and Y.-H. Lin, "Second-order scattering induced reflection divergence and nonlinear depolarization on randomly corrugated semiconductor nano-pillars," *Progress In Electromagnetics Research,* Vol. 117, 67–81, 2011.
23. Wang, X. and L.-W. Li, "Numerical characterization of bistatic scattering from PEC cylinder partially embedded in a dielectric

rough surface interface: Horizontal polarization," *Progress In Electromagnetics Research*, Vol. 91, 35–51, 2009.

24. Hohn, D. H., "Depolarization of a Laser Beam at 6328 A due to Atmospheric Transmission," *J. Appl. Opt.*, Vol. 8, 367–369, 1969.
25. Gil, J. J. and E. Bernabeu, "A depolarization criterion in Mueller matrices," *Opt. Acta*, Vol. 32, 259–261, 1985.
26. Gil, J. J. and E. Bernabeu, "Depolarization and polarization indices of an optical system," *Opt. Acta*, Vol. 33, 185–189, 1986.
27. Chipman, R. A., "Depolarization index and the average degree of polarization," *J. Appl. Opt.*, Vol. 44, 2490–2495, 2005.
28. Zhu, S. and Y. Cai, "Degree of polarization of a twisted electromagnetic Gaussian Schell-model beam in a Gaussian cavity filled with gain media," *Progress In Electromagnetics Research B*, Vol. 21, 171–187, 2010.
29. Clifford, S. F. and H. T. Yura, "Equivalence of two theories of strong optical scintillation," *J. Opt. Soc. Am.*, Vol. 64, 1641–1644, 1974.
30. Holmes, J. F., H. L. Myung, and J. R. Kerr, "Effect of the log-amplitude covariance function on the statistics of speckle propagation through the turbulent atmosphere," *J. Opt. Soc. Am.*, Vol. 70, 355–360, 1979.
31. ITU-R. Document 3J/31-E, "On propagation data and prediction methods required for the design of space-to-earth and earth-to-space optical communication systems," *Radio Communication Study Group Meeting, Budapest*, Vol. 206, 277–293, 2001.
32. Zhao, X. H., Y. Yao, Y. X. Sun, and C. Liu, "Condition for Gaussian Schell-model beam to maintain the state of polarization on the propagation in free space," *J. Opt. Soc. Am.*, Vol. 17, 88–94, 2009.